

## ARTICLES

**Dynamics for Solubilization of Naphthalene and Pyrene into *n*-Decyltrimethylammonium Perfluorocarboxylate Micelles**Nobuyuki Yoshida,<sup>†</sup> Yoshikiyo Moroi,<sup>\*,†</sup> Robin Humphry-Baker,<sup>‡</sup> and Michael Grätzel<sup>‡</sup>*Chemistry and Physics of Condensed Matter, Graduate School of Sciences, Kyushu University-Ropponmatsu, Fukuoka 810-8560, Japan, and Institut de Chimie Physique II, Ecole Polytechnique Federal de Lausanne, CH-1015, Lausanne, Switzerland**Received: October 15, 2001; In Final Form: January 31, 2002*

The entry and exit rate constants of naphthalene and pyrene to and from a micelle ( $k_+$  and  $k_-$ , respectively) have been determined for *n*-decyltrimethylammonium trifluoroacetate (DeTAPA) and pentafluoropropionate (DeTAPP) micelles by a steady-state fluorescence quenching method. The  $k_-$  values of naphthalene and pyrene for DeTAPA micelles increased with increasing temperature, whereas the values from DeTAPP micelles had a minimum at 308.2 K. The  $k_+$  values of naphthalene and pyrene to DeTAPA micelles also increased with increasing temperature, whereas the values for DeTAPP micelles again showed a minimum at the same temperature. The fluorescence spectra of pyrene have indicated that the molecule is located at the hydrophilic outer site in DeTAPA and DeTAPP micelles rather than at the hydrophobic micellar core site.

**Introduction**

Fluorescence quenching methods have been well proven to probe the microenvironmental properties of micellar and polymer solutions in an aqueous system.<sup>1</sup> Moreover, the method has been applied to investigations of biological systems such as aggregation behavior of bile salts, mechanism of photosynthesis, and interaction between proteins and drugs.<sup>2-6</sup> In particular, pyrene and its derivatives have been shown to be useful photoprobes, since the excited states are relatively stable and the excited molecules can easily form an excimer in condensed phases. Indeed, they have been widely employed as probe molecules for photochemical processes in micellar solutions and polymers in aqueous solution.<sup>7,8</sup>

Time-resolved fluorescence quenching methods and steady-state fluorescence quenching methods have provided insight into

the microscopic nature of small aggregates.<sup>9</sup> The former measures the lifetime of the probe in aggregates, which indicates the extent of the interaction between the probe and the matrix. In addition, with the use of an appropriate quencher, it can further derive important microscopic information such as the micelle aggregation number.<sup>10</sup> The latter also provides information on the molecular aggregates and on the mobility of probe and the interaction with a quencher in the aggregates,<sup>11</sup> which can also lead to the aggregation number. Information obtained by the former and latter methods often complements each other.<sup>12,13</sup>

The first stepwise association constant for solubilization ( $\bar{K}_1$ ) between a micelle and a solubilize can be determined by application of solubilization model.<sup>14</sup> The authors have studied the thermodynamic properties on several solubilization systems to determine the first stepwise association constants between a polycyclic aromatic compound and a vacant micelle. They use this approach in the first half of this study. From the thermodynamic point of view, the association constant indicates the

\* Author to whom correspondence should be addressed. Fax: 81-92-726-4842. E-mail: moroiscc@mbox.nc.kyushu-u.ac.jp.

<sup>†</sup> Kyushu University-Ropponmatsu.

<sup>‡</sup> Ecole Polytechnique Federal de Lausanne.

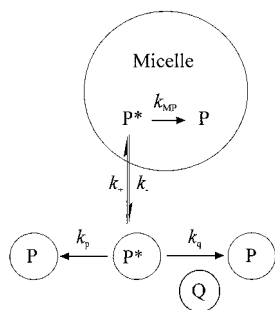


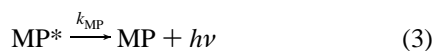
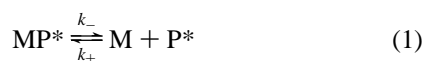
**Figure 1.** Scheme of the fluorescence quenching method.

capability of a micelle to incorporate a solubilize and gives, at the same time, the ratio of the entry rate constant into a vacant micelle ( $k_+$ ) to the escape rate constant from the micelle ( $k_-$ ) for a solubilize molecule. Hence, if either rate constant can be determined, the other can be automatically evaluated from this constant.

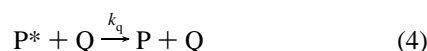
One of the purposes of this study is to present a theoretical expression for the rate constant determination in a micellar system by the steady-state fluorescence quenching method. The other is a quantitative description of the dynamics of solubilization. The discussion will be made on the relationship between the rate constant and the hydrophobicity of micelles for two anionic and two cationic surfactant systems.

### Theory

The value of  $\bar{K}_1$  is an indicator for the magnitude of interaction between a micelle and a solubilize.<sup>15</sup> The constant is also regarded as the ratio of the entry rate constant ( $k_+$ ) of a solubilize into a micelle to the exit rate constant ( $k_-$ ) from the micelle. In the present case, the association constant  $\bar{K}_1$  is obtained from fluorescence photo probes in the micellar solution. Under steady-state irradiation the excited probe P in a micelle,  $MP^*$  loses energy via the following processes (Figure 1):



Equation 1 is the first stepwise association equilibrium. Equations 2 and 3 indicate the radiative decay of the excited probe in intermicellar bulk and that associated with the micelle, respectively, and include inherent quenching modes other than spontaneous emission. If a water-soluble quencher Q is added to such a system, the fluorescence intensity would decrease due to excited-state quenching as long as the photoprobe P can escape from the micelle, where



should be the only effective quenching reaction in the solution.

The above decrease in fluorescence intensity should have a relationship with the quencher concentration as expanded below. Equations 1–4 construct the following two differential equations for the kinetics of  $[MP^*]$  and  $[P^*]$ :

$$\frac{d[MP^*]}{dt} = I_a^{MP} + k_+[M][P^*] - k_-[MP^*] - k_{MP}[MP^*] \quad (5)$$

$$\frac{d[P^*]}{dt} = I_a^P + k_-[MP^*] - k_+[M][P^*] - k_p[P^*] - k_q[P^*][Q] \quad (6)$$

Here,  $I_a^{MP}$  and  $I_a^P$  are the incident photon flux for exciting the fluorescence probe in micelle and in bulk water, respectively. At steady-state,

$$I_a^{MP} = (k_- + k_{MP})[MP^*] - k_+[M][P^*] \quad (7)$$

$$I_a^P = (k_+[M] + k_p + k_q[Q])[P^*] - k_-[MP^*] \quad (8)$$

Assuming that the rates  $I_a^{MP}$  and  $I_a^P$  are proportional to the corresponding excited probe concentration, that is,

$$\frac{I_a^P}{I_a^{MP}} = \frac{[P^*]}{[MP^*]} \quad (9)$$

the following relation between  $[P^*]$  and  $[MP^*]$  would be obtained from eqs 7–9:

$$\frac{[P^*]}{[MP^*]} = \frac{-k([Q]) + \sqrt{\{k([Q])\}^2 + 4k_-k_+[M]}}{2k_+[M]} = A([Q]) \quad (10)$$

where

$$k([Q]) = k_p - k_{MP} + k_+[M] - k_- + k_q[Q] \quad (11)$$

and  $A([Q])$  is a function of  $[Q]$ . The quantum yield  $\Phi$  can be then obtained:

$$\Phi = \frac{k_{MP}[MP^*] + k_p[P^*]}{I_a^{MP} + I_a^P} = \frac{k_{MP} + k_p \frac{[P^*]}{[MP^*]}}{k_{MP} + (k_p + k_q[Q]) \frac{[P^*]}{[MP^*]}} = \frac{k_{MP} + k_p A([Q])}{k_{MP} + (k_p + k_q[Q]) A([Q])} \quad (12)$$

Without quencher, the yield  $\Phi^\circ$  becomes unity:

$$\Phi^\circ = \frac{k_{MP}[MP^*] + k_p[P^*]}{(I_a^{MP} + I_a^P)_{[Q]=0}} = 1 \quad (13)$$

Finally, the ratio of the total fluorescence intensities in the absence to the presence of quencher is given by the following equation:

$$\phi = \frac{\Phi^\circ}{\Phi} = 1 + \frac{k_q[Q]A([Q])}{k_{MP} + k_p A([Q])} \quad (14)$$

The  $k_-$  and  $k_+$  values can then be obtained from the plots of  $\phi$  vs quencher concentration  $[Q]$ .

### Experimental Section

**Materials.** *n*-Decyltrimethylammonium trifluoroacetate (DeTAPA) and *n*-decyltrimethylammonium pentafluoropropionate (DeTAPP) were synthesized as described in the previous paper.<sup>16</sup> Naphthalene and pyrene were purified by the same method as in the previous study.<sup>17</sup> *n*-Hexane of guaranteed reagent grade (97%) from Nacalai Tesque was used without any further purification. Silver(I) trifluoroacetate ( $CF_3COOAg$ ) was also synthesized and purified by a previous method.<sup>16</sup>

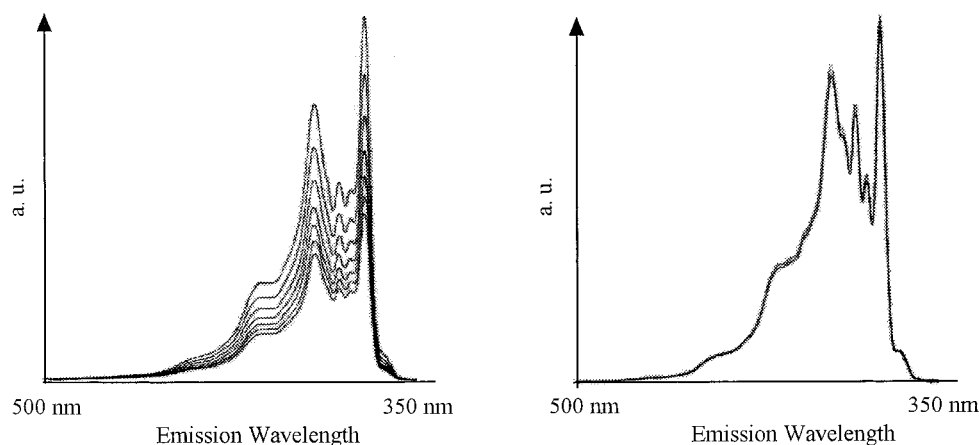


**Figure 2.** Fluorescence spectra of pyrene at 298.2 K with adding  $C_2F_5COOAg$  solution: (a) in water, (b) in DeTAPP solution.

Silver(I) pentafluoropropionate ( $C_2F_5COOAg$ ) was obtained from Aldrich and used without further purification.

**Steady-State Fluorescence Quenching Method.** The decay rate constants ( $k_p$ ) of naphthalene and pyrene in an aqueous solution were  $2.34 \times 10^7 \text{ s}^{-1}$  and  $7.07 \times 10^6 \text{ s}^{-1}$  at room temperature, respectively, which were independently obtained in the previous study.<sup>18</sup> The decay rate constants  $k_{MP}$  in a micelle were also determined by a time-resolved single photon counting method using a  $H_2$  source lamp for the micellar solution containing a probe molecule at the most. The excitation and emission wavelengths were 280 and 320 nm, respectively, for naphthalene and 350.7 and 392 nm for pyrene. The micellar concentration was ca.  $1 \times 10^{-3} \text{ mol dm}^{-3}$  for each solution, and the probe concentration was ca.  $6 \times 10^{-6} \text{ mol dm}^{-3}$  for both naphthalene and pyrene. The decay rate constant of an excited anthracene molecule has been also determined ( $k_p = 2.70 \times 10^8 \text{ s}^{-1}$ ) in the previous paper.<sup>18</sup> However, the authors did not attempt to determine the entry and the exit rate constants for anthracene, since the  $k_p$  value is too large to detect any quenching by  $Ag^+$  in micellar solutions.

For the steady-state fluorescence quenching measurement, the aqueous solution of each fluorescence probe was prepared by dilution of the respective saturated solutions for naphthalene and pyrene at room temperature. Such dilute concentrations did not disturb the precise determination of efficient emission intensity of the probe themselves. The final probe concentrations were  $5.0 \times 10^{-6} \text{ mol dm}^{-3}$  for naphthalene and  $1.8 \times 10^{-7} \text{ mol dm}^{-3}$  for pyrene, which were checked by UV-vis spectrophotometry. These concentrations are less than their aqueous solubility:  $2.1 \times 10^{-4}$  and  $3.9 \times 10^{-7} \text{ mol dm}^{-3}$  at 298.2 K for naphthalene and pyrene, respectively. These solutions were also used for the determination of  $k_q$  in water. The micellar solutions were prepared by adding solid surfactant to the probe aqueous solution to have a final micellar concentration ( $[M]$ ) of ca.  $1 \times 10^{-3} \text{ mol dm}^{-3}$  at temperatures from 288.2 to 318.2 K. It has been reported that the solubilized pyrene molecules perturb the micellar size at high pyrene concentration or high counterion salt concentration.<sup>19,20</sup> Therefore, the experiments were performed at low pyrene and quencher concentrations. These solutions were also used for the determination of the rate constants. The quencher solutions were prepared by using the above probe stock solutions in order for the composition not to change, when the quencher was introduced into the experimental system.

Steady-state fluorescence intensities in DeTAPA and DeTAPP micellar solution were measured by a fluorescence spectrophotometer (Hitachi model 650-60) at temperatures from 288.2

to 318.2 K, where the temperature was maintained constant by circulating temperature-controlled water around the photocell.<sup>18</sup> The excitation wavelengths are 276 and 336 nm for naphthalene and pyrene, respectively, which are the most effective wavelengths for excitation of each fluorescent probe. The emission intensity was recorded from 300 to 450 nm and from 350 to 500 nm for naphthalene and pyrene, respectively, where the excitation slit width was 5 nm and the emission slit width was 1.5 nm. The emission intensity as a function of quencher concentration was observed at 326 nm for naphthalene and at 375 nm for pyrene at their respective emission maxima.

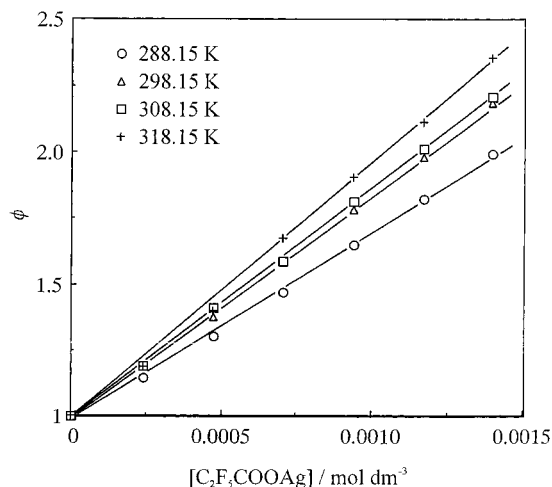
The intensity ratios of peaks at 385 and 375 nm for pyrene in the above temperature range were also evaluated from the emission spectra in DeTAPA and DeTAPP micellar solutions to obtain the so-called  $I_{III}/I_I$  ratio in the solubilized state between 288.2 and 323.2 K.<sup>21</sup>

## Results and Discussion

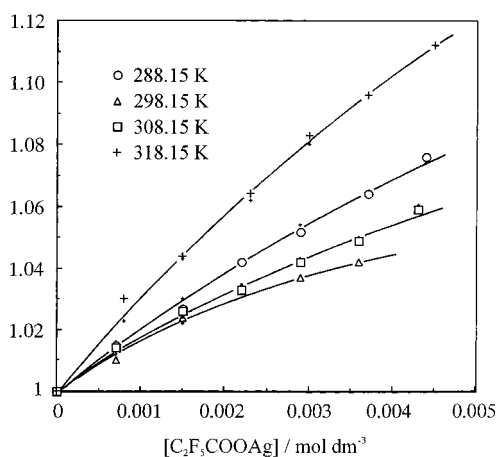
**Kinetic Parameters for Solubilization.** The lifetime of naphthalene in both DeTAPA and DeTAPP micelles was observed to be  $8.54 \times 10^{-8} \text{ s}$ , whereas that one of pyrene was  $1.76 \times 10^{-7}$  and  $1.78 \times 10^{-7} \text{ s}$  in DeTAPA and DeTAPP micelles, respectively. The parameters for each probe agreed well within 2%. The decay rate constant  $k_{MP}$  thus obtained was  $1.17 \times 10^7 \text{ s}^{-1}$  for naphthalene in both anionic micellar solutions and  $5.69 \times 10^6$  and  $5.61 \times 10^6 \text{ s}^{-1}$  for pyrene in DeTAPA and DeTAPP micellar solution, respectively.

Figure 2 illustrates the change in spectra of pyrene in water and in DeTAPP micellar solution with increasing concentration of quencher. The intensity of the peak decreased upon stepwise addition of quencher in both solutions. The cationic micelles keep cationic quencher ( $Ag^+$ ) away from micelles by the electrostatic repulsion and prevent the quenching of the excited probe from taking place within the micelle, although a small part of the probe is quenched outside of the micelle. Therefore, the  $Ag^+$  quenching effect should be reduced when the fluorophore is protected by micelle compared to that in water.

Atmospheric oxygen easily dissolves into aqueous and micellar solutions, and molecular oxygen is in general an effective quencher for the fluorescent hydrocarbon probes.<sup>1,22</sup> The kinetics of fluorescence quenching by oxygen has been thoroughly studied,<sup>23</sup> and the quenching rate constant has also been determined for some probes in various solvents.<sup>24</sup> However, the effect of oxygen was not apparently considered in this study, since it is hard to estimate the oxygen effect on the quenching rate constants, and at the same time, the effect has



**Figure 3.** The Stern–Volmer plots for determination of the quenching rate constants  $k_q$  of pyrene by  $C_2F_5COOAg$  in water at temperatures from 288.2 to 318.2 K.



**Figure 4.** The Stern–Volmer plots for determination of  $k_-$  and  $k_+$  values of pyrene in DeTAPP micellar solution at temperatures from 288.2 to 318.2 K. The solid curves are the calculated fit data from eq 14.

been already included in the  $k_p$ ,  $k_{MP}$ , and  $k_q$  values. In other words, the whole rate constants are those for air-saturated solutions.

Quenching rate constants  $k_q$  of the probe by each quencher ( $CF_3COOAg$  and  $C_2F_5COOAg$ ) in water and in micellar solution were determined from the Stern–Volmer plots (Figures 3 and 4). The quenching rate constant for  $Ag^+$  was also determined over the temperature range from 288.2 to 318.2 K. (Tables 1 and 2). As is expected, the constants increase with increasing temperature due to the increasing rates of diffusion.

A number of studies with ionic quenchers such as bromide ion or pyridinium ion showed no quenching of the fluorescence of aromatic compounds solubilized into micelles having the same charge as the ionic micelles.<sup>25–27</sup> It is quite reasonable that the lifetime of the hydrophobic fluorescence probes could not be shortened by adding the above quenchers to micellar solutions, since the quenchers cannot come close to the solubilized probe in a micelle because of the electrostatic repulsion. If most probes are assumed to exist in the micelles<sup>28</sup> and if their exit rate constant is much smaller than the fluorescence decay rate constant during the period of time for the time-resolved fluorescence quenching, then the excited probe would return to its ground state with the emission light before it escapes from the micelle or without giving the activated energy to the quencher in inter-micellar bulk. The steady-state

fluorescence intensity, however, decreases slightly by adding the quencher into the solution, since the excitation light is always exposed to the solution and there must exist some dissociated probe molecules under equilibrium conditions. The measured emission spectra were truly governed by the quencher concentration. This fact indicates that a small but finite number of probes exists freely in the bulk, as the first stepwise association constant  $\bar{K}_1$  can be determined from the solubilization experiments.

The authors will consider the interaction between the probes and the micelles through the process of derivation of the association constants. Exit and entry rate constants have been determined for many chemical species used as a quencher molecule by the time-resolved fluorescence quenching measurements.<sup>29</sup> The  $k_-$  values for fluorescence probe, however, have not been determined in any paper except the study by Almgren et al.,<sup>30</sup> where the  $k_+$  value was determined from the solubilization of 1-bromonaphthalene into a SDS micelle, and the value was  $5\text{--}8 \times 10^9 \text{ mol}^{-1} \text{ dm}^3 \text{ s}^{-1}$  from the apparent lifetime in the micellar solution using  $NaNO_2$  as a quencher. The  $k_+$  values were used to derive the exit rate constants  $k_-$  for other probes such as naphthalene and pyrene, since the  $k_+$  value should be independent of chemical species if the mechanism were diffusion-controlled.

For the case of pyrene in DeTAPA and DeTAPP micellar solutions, substituting the diffusion-controlled  $k_q$  value for  $k_+$  value in eq 14 did not give a good curve fit. Therefore, both  $k_+$  and  $k_q$  were optimized as parameters to produce a good curve fit. The entry rate constants of pyrene into DeTAPA and DeTAPP were much larger than those of naphthalene at all temperatures (Tables 1 and 2). Therefore, the interaction between the micelle and the pyrene molecule has effectively increased the constant  $k_+$  due to strong interaction between the headgroup of surfactant and the probe molecule, as has been reported before.<sup>31,32</sup>

The  $k_-$  values thus obtained are plotted against temperature for naphthalene and pyrene in DeTAPA and DeTAPP solution (Figures 5 and 6). The value of naphthalene was larger by 1 order of magnitude than that of pyrene, since escape tendency of solubilize should decrease with increasing hydrophobicity. Slight increase of  $k_-$  values with increasing temperature from DeTAPA micelle reflects the decrease in the micellar size and in the hydrophobic interaction between micelle and solubilize. In DeTAPP solution, however, the  $k_-$  and  $k_+$  values suddenly increased for both probe solubilizes at 318.2 K despite the decrease in micellar size. This change corresponds to a sudden increase in the degree of counterion binding to micelle as reported in the previous paper<sup>33</sup> and suggests the possibility of a drastic change of structure around the micellar surface.

The  $k_+$  of pyrene, on the other hand, is larger than that of naphthalene (Figures 7 and 8). This difference might be the consequence of the interaction model used for the solubilization. The first stepwise association constant  $\bar{K}_1$  was defined as the equilibrium constant of the first stepwise solubilization reaction in eq 1, where a small aggregate formed by a small number of monomer and solubilize molecules were not taken into consideration. The aqueous solubility of the solubilize, pyrene, increased slightly with surfactant concentration below the cmc, which suggests an interaction between pyrene and surfactant. Such an increase was not observed for naphthalene. If this interaction was considered, for example, in the case of solubilization of pyrene in DeTAPP solution at 298.2 K,<sup>16</sup> the following calculations would show that  $[pyrene] = 0.796 \mu\text{M}$  at the cmc from extrapolation of the solubility below cmc

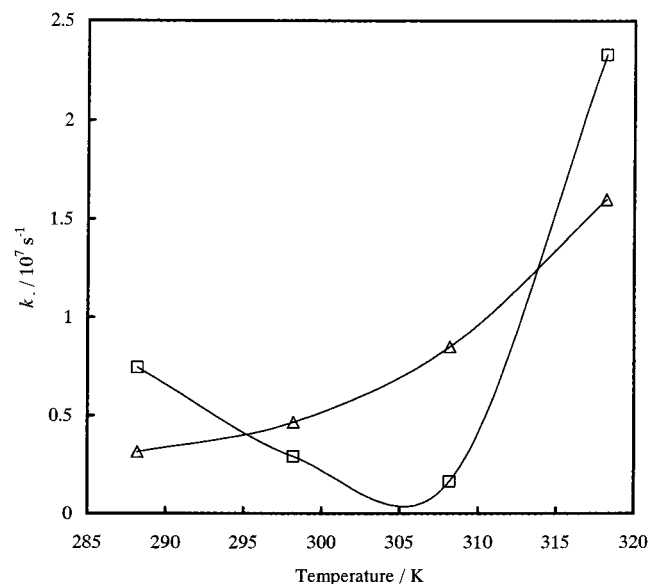
TABLE 1: Kinetic Parameters for Solubilization of Naphthalene

$T$ (K)	$\bar{K}_1$ ( $\text{mol}^{-1} \text{dm}^3$ )	$k_q$ ( $\text{mol}^{-1} \text{dm}^3 \text{s}^{-1}$ )	$k_q$ (cf) <sup>a</sup> ( $\text{mol}^{-1} \text{dm}^3 \text{s}^{-1}$ )	$k_-$ ( $\text{s}^{-1}$ )	$k_+$ ( $\text{mol}^{-1} \text{dm}^3 \text{s}^{-1}$ )
DeTAPA					
288.2	$2.65 \times 10^4$	$4.52 \times 10^9$	$4.52 \times 10^9$	$3.16 \times 10^6$	$8.37 \times 10^{10}$
298.2	$2.09 \times 10^4$	$5.67 \times 10^9$	$9.30 \times 10^9$	$4.67 \times 10^6$	$9.77 \times 10^{10}$
308.2	$1.42 \times 10^4$	$7.20 \times 10^9$	$1.26 \times 10^{10}$	$8.52 \times 10^6$	$1.21 \times 10^{11}$
318.2	$1.00 \times 10^4$	$7.58 \times 10^9$	$1.53 \times 10^{10}$	$1.60 \times 10^7$	$1.60 \times 10^{11}$
DeTAPP					
288.2	$4.45 \times 10^4$	$3.81 \times 10^9$	$1.51 \times 10^9$	$7.44 \times 10^6$	$3.31 \times 10^{11}$
298.2	$2.35 \times 10^4$	$4.11 \times 10^9$	$4.11 \times 10^9$	$2.91 \times 10^6$	$6.83 \times 10^{10}$
308.2	$1.73 \times 10^4$	$6.96 \times 10^9$	$6.96 \times 10^9$	$1.63 \times 10^6$	$2.86 \times 10^{10}$
318.2	$1.22 \times 10^4$	$7.90 \times 10^9$	$7.90 \times 10^9$	$2.33 \times 10^7$	$2.84 \times 10^{11}$

<sup>a</sup> Values from curve fitting.

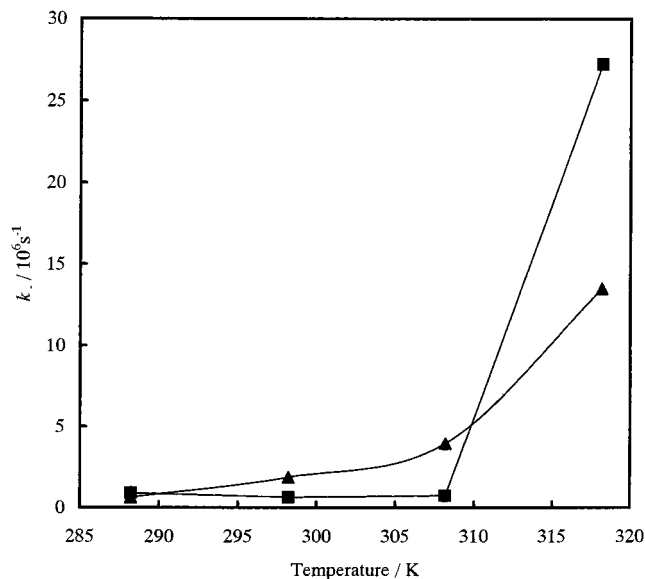
TABLE 2: Kinetic Parameters for Solubilization of Pyrene

$T$ (K)	$\bar{K}_1$ ( $\text{mol}^{-1} \text{dm}^3$ )	$k_q$ ( $\text{mol}^{-1} \text{dm}^3 \text{s}^{-1}$ )	$k_q$ (cf) <sup>a</sup> ( $\text{mol}^{-1} \text{dm}^3 \text{s}^{-1}$ )	$k_-$ ( $\text{s}^{-1}$ )	$k_+$ ( $\text{mol}^{-1} \text{dm}^3 \text{s}^{-1}$ )
DeTAPA					
288.2	$2.69 \times 10^6$	$3.88 \times 10^9$	$3.80 \times 10^{11}$	$6.44 \times 10^5$	$1.73 \times 10^{12}$
298.2	$1.53 \times 10^6$	$5.33 \times 10^9$	$1.74 \times 10^{11}$	$1.86 \times 10^6$	$2.85 \times 10^{12}$
308.2	$8.84 \times 10^5$	$5.95 \times 10^9$	$1.40 \times 10^{11}$	$3.96 \times 10^6$	$3.50 \times 10^{12}$
318.2	$5.19 \times 10^5$	$7.02 \times 10^9$	$1.17 \times 10^{11}$	$1.35 \times 10^7$	$7.00 \times 10^{12}$
DeTAPP					
288.2	$3.69 \times 10^6$	$4.94 \times 10^9$	$1.09 \times 10^{10}$	$9.02 \times 10^5$	$5.34 \times 10^{12}$
298.2	$2.30 \times 10^6$	$5.94 \times 10^9$	$3.26 \times 10^{11}$	$6.29 \times 10^5$	$1.54 \times 10^{12}$
308.2	$8.99 \times 10^5$	$6.11 \times 10^9$	$3.39 \times 10^{11}$	$7.42 \times 10^5$	$8.09 \times 10^{11}$
318.2	$5.43 \times 10^5$	$6.76 \times 10^9$	$8.40 \times 10^{10}$	$2.72 \times 10^7$	$1.10 \times 10^{13}$

<sup>a</sup> Values from curve fitting.Figure 5. Exit rate constant  $k_-$  of naphthalene molecule from DeTAPA ( $\Delta$ ) and DeTAPP ( $\square$ ) micelles at temperatures from 288.2 to 318.2 K.

([pyrene] = 0.390  $\mu\text{M}$  in the case of surfactant free),  $\bar{K}_1 = 6.72 \times 10^5 \text{ mol}^{-1} \text{dm}^3$ ,  $k_- = 5.98 \times 10^5 \text{ s}^{-1}$ , and  $k_+ = 4.02 \times 10^{11} \text{ mol}^{-1} \text{dm}^3 \text{s}^{-1}$  by curve fitting according to eq 14 ( $k_q = 7.57 \times 10^{10} \text{ mol}^{-1} \text{dm}^3 \text{s}^{-1}$ ). In this case, the pyrene molecule associated with surfactant ions was regarded as a pyrene monomer locating outside the micelle. The value of  $k_+$  becomes much smaller than the previous one, whereas the  $k_-$  value showed almost no change.

A slight increase of the  $k_-$  values with increasing temperature for the DeTAPA micelles reflects easy escape of the probe molecule due to the decrease in the micellar size and in hydrophobic interaction between the micelle and probe. In DeTAPP solution, however, the  $k_-$  and  $k_+$  values increased

Figure 6. Exit rate constant  $k_-$  of pyrene molecule from DeTAPA ( $\Delta$ ) and DeTAPP ( $\blacksquare$ ) micelles at temperatures from 288.2 to 318.2 K.

suddenly for naphthalene and pyrene at 318.2 K despite a decrease in its micellar size. This change corresponds to a sudden increase in the degree of counterion binding to micelle as reported in the previous paper and suggests the possibility of a drastic change of structure around the micellar surface.

In the previous paper,<sup>18</sup> two adjustable parameters,  $k_q$  and  $k_-$ , were necessary to trace the relationships between the fluorescence ratio  $\Phi^\circ/\Phi$  and  $[Q]$  for the determination of the entry and the exit rate constants of naphthalene and pyrene into *n*-dodecylammonium trifluoroacetate ( $\text{C}_{12}\text{H}_{25}\text{NH}_4^+ \text{CF}_3\text{COO}^-$ ). In addition, the  $k_q$  value obtained was much larger than the ones found from the Stern–Volmer plots. In this study too, the same results were obtained despite using a different set of assumptions

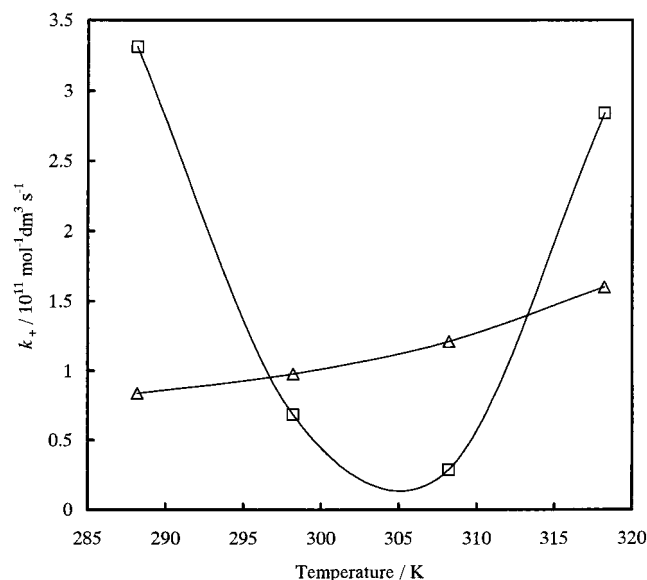


**Figure 7.** Entry rate constant  $k_+$  of naphthalene molecule from DeTAPA ( $\Delta$ ) and DeTAPP ( $\square$ ) micelles at temperatures from 288.2 to 318.2 K.

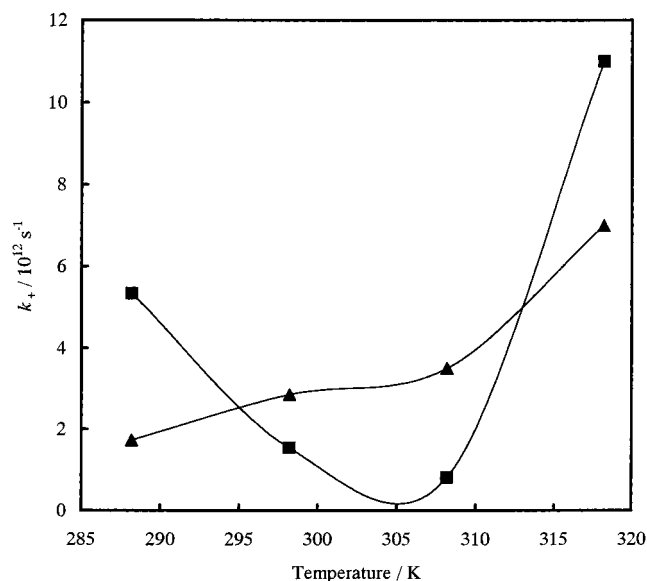


**Figure 8.** Entry rate constant  $k_+$  of pyrene molecule from DeTAPA ( $\blacktriangle$ ) and DeTAPP ( $\blacksquare$ ) micelles at temperatures from 288.2 to 318.2 K.

(eq 9), which was noticeable for pyrene. The  $k_+$  values were also much larger than expected from a diffusion-controlled reaction, even though surface area of the micelle with which a solubilize molecule collides was more than 10 times larger than a reaction area of a common chemical species. The larger values of  $k_q$  and  $k_+$ , especially for pyrene, can be explained by location of the solubilize and the quencher  $\text{Ag}^+$  in close proximity to the micelles or a static quenching by  $\text{Ag}^+$ .<sup>34</sup>

#### Solubilization Site of a Pyrene Molecule

Pyrene fluorescence has often been used as an index for the microenvironment of the solubilization site.<sup>35</sup> The fluorescence intensities of the O–O vibronic bands depend on solvents, and the intensity ratio of peaks III to I decreases with increasing dielectric constant of the medium around the probe molecule.<sup>36</sup> This phenomenon was drawn from the analogy to the well-known Ham effect<sup>37</sup> which resulted from dispersion force perturbation by the solvent molecules. The intensity ratio then

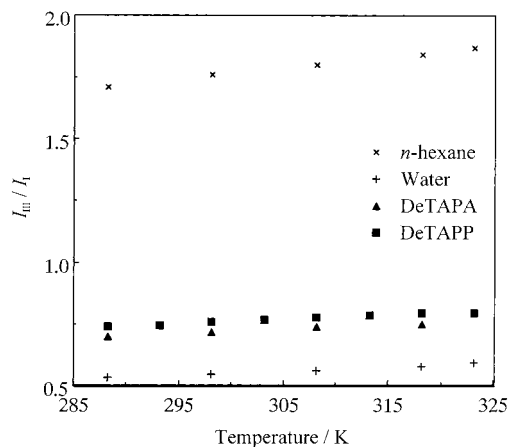


**Figure 9.** Change of the ratio of fluorescence intensity ( $I_{\text{III}}/I_{\text{I}}$ ) of pyrene with temperature in  $n$ -hexane, water, DeTAPA, and DeTAPP micellar solutions.

reflects the polarity of solvent molecules around the probe molecule.<sup>38,39</sup> In this sense, pyrene is the most powerful probe molecule for study on colloid and interface science, although there are many other probes which can be used as an indicator of the solvent polarity.<sup>40</sup>

The ratio of fluorescence intensities at 385 and 375 nm of pyrene were measured in water,  $n$ -hexane, DeTAPA, and DeTAPP solutions (Figure 9). The fluorescence intensity decreased with quencher concentration, but the  $I_{\text{III}}/I_{\text{I}}$  ratio remained almost constant. This confirms that the micellar structure and the site of the pyrene molecule in the micelles remain almost the same in the presence of small amounts of quencher. The ratio was found to be almost independent of temperature for the surfactants used and indicated that the pyrene molecule solubilized into a micelle is located at a slightly more hydrophobic site for the DeTAPP micelles than for DeTAPA micelles (Figure 9). The present figure clearly indicates that the aromatic probe is solubilized near the micellar surface or in a palisade layer of micelles on average, as inferred from the previous studies.<sup>31,32</sup> It is not possible to insist that the pyrene molecule is solubilized at the inner micellar core, since the hydrophobicity of the micellar counterions is directly affecting the ratio. The difference in the ratio, however, could be one of the reasons to explain the difference in  $k_-$  between DeTAPA and DeTAPP micelles. This phenomenon could be used to explain the difference in hydrophobic interaction between both micelles. That is, the value of  $k_-$  of the aromatic compounds was larger for DeTAPA micelles than for DeTAPP below 318.2 K, since the hydrophobic interaction controlled the exit rate from the micelles.

The kinetic parameters and the  $I_{\text{III}}/I_{\text{I}}$  ratio suggest that the pyrene molecule is located at a similar site in DeTAPA and DeTAPP micelles over the temperature range examined. This is reasonable, since the exit and entry rate constants for all the species in the micelles—surfactant ion, counterion, and solubilizes—were of similar order. These species undergo rapid exchange between a micelle and the inter-micellar bulk under equilibrium conditions. The rate constants for solubilization of other aromatic compounds also support this fast change of structure around the micellar surface.<sup>31</sup>

Differences in hydrophobic environment of the solubilization site between DeTAPA and DeTAPP micelles would come from the difference in hydrophobicity of the counterion themselves. Since decane sulfonic acid (DSA) and sodium decane sulfonate (SDeSo) molecules have a similar headgroup to sodium dodecyl sulfate (SDS), a pyrene molecule locates in a similar inner site

in these micelles, which was supported by the values of  $I_{III}/I_I$  in these micelles at 308.2 K: 0.87 for SDeSo and 0.84 for SDS. Thus, the exit rate constants  $k_-$  from DSA and SDeSo micelles<sup>36</sup> should be smaller than those of DeTAPA and DeTAPP. However, the results were not conclusive. The same arguments could be made for naphthalene, although the interaction of this probe with DeTAPA and DeTAPP headgroups should be weaker than that of pyrene. In short, the difference in the exit rate constant among the present micelles could be explained by (1) the extent of hydrophobic interaction between micelle and solubilize, and (2) the difference in the solubilization site of fluorescence probe in micelles.

## Conclusion

The entry and exit rate constants for solubilization of naphthalene and pyrene into and from the cationic micellar solutions were determined by the steady-state fluorescence quenching method. The  $k_-$  values were clearly dependent on the strength of hydrophobic interaction between micelles and aromatic probe solubilizes, which also explained the sudden change of DeTAPP micellar surface appearing at 318.2 K. The  $k_+$  values of pyrene into DeTAPA and DeTAPP micelles were much larger than those of naphthalene and than the one of pyrene into SDeSo micelles, which suggests the strong interaction of pyrene molecule with headgroups of the cationic micelles. It became possible from this study to detect transformation of surface structure in a micelle by using an appropriate fluorescence probe which locates around the micellar surface and by using a quencher which can approach the micelles despite electrostatic repulsion. Molecular interaction between probe and nonmicellar surfactant becomes conclusive for the solubilization constant, and at the same time, change in temperature brings about a drastic change in aggregates system.

**Acknowledgment.** This work was partly supported by a Giant-in-Aid for Scientific Research No. 10554040 from the Ministry of Education, Science and Culture, Japan, which is gratefully acknowledged.

## References and Notes

- (1) Turro, N. J.; Grätzel, M.; Braun, A. M. *Angew. Chem., Int. Ed. Engl.* **1980**, *19*, 675–696.
- (2) Hashimoto, S.; Thomas, J. K. *J. Colloid Interface Sci.* **1997**, *102*, 152–163.
- (3) Zana, R.; Guveli, D. *J. Phys. Chem.* **1985**, *89*, 1687–1690.
- (4) Schweitzer, R. H.; Brudvig, G. W. *Biochemistry* **1997**, *36*, 11351–11359.
- (5) Wassenberg, D.; Liebl, W.; Jaenicke, R. *J. Mol. Biol.* **2000**, *295*, 279–288.
- (6) Trivedi, V. D.; Vorum, H.; Honoré, B.; Qasim, M. A. *J. Pharm. Pharmacol.* **1999**, *51*, 591–600.
- (7) Mizusaki, M.; Morishima, Y.; Yoshida, K.; Dubin, P. L. *Langmuir* **1997**, *13*, 6941–6946.
- (8) In, M.; Bec V.; Aguerre-Chariol, O.; Zana, R. *Langmuir* **2000**, *16*, 141–148.
- (9) Infelta, P. P. *Chem. Phys. Lett.* **1979**, *61*, 88–91.
- (10) Szajdzinska-Pietek, E.; Wolszczak, M. *Langmuir* **2000**, *16*, 1675–1680.
- (11) Asakawa, T.; Amada, K.; Miyagishi, S. *Langmuir* **1997**, *13*, 4569–4573.
- (12) Jover, A.; Meijide, F.; Núñez, E. R.; Tato, J. V.; Mosquera, M. *Langmuir* **1997**, *13*, 161–164.
- (13) Alargova, R. G.; Kochijashky, I. I.; Sierra, M. L.; Zana, R. *Langmuir* **1998**, *14*, 5412–5418.
- (14) Moroi, Y. *Micelles: Theoretical and Applied Aspects*; Plenum Press: New York, 1992.
- (15) Yoshida, N.; Moroi, Y. *J. Colloid Interface Sci.* **2000**, *232*, 33–38.
- (16) Yoshida, N.; Matsuoka, K.; Moroi, Y. *J. Colloid Interface Sci.* **1997**, *187*, 388–395.
- (17) Moroi, Y.; Mitsunobu, K.; Morisue, T.; Kadobayashi, Y.; Sakai, M. *J. Phys. Chem.* **1995**, *99*, 2372–2376.
- (18) Moroi, Y.; Morisue, T.; Matsuo, H.; Yonemura, H.; Humphry-Baker, R.; Grätzel, M. *J. Chem. Soc., Faraday Trans.* **1997**, *93*, 3345–3349.
- (19) Offen, H. W.; Dawson, D. R.; Nicoli, D. F. *J. Colloid Interface Sci.* **1981**, *80*, 118–122.
- (20) Almgren, M.; Swarup, S. *J. Phys. Chem.* **1982**, *86*, 4212–4216.
- (21) Kalyanasundaram, K. *Photochemistry in Organized & Constrained Media*; Rammurthy, V., Ed.; VCH Publishers: New York, 1991.
- (22) Moroi, Y. *Adv. Colloid Interface Sci.* **1997**, *73*, 47–69.
- (23) Birks, J. B. *Photophysics for Aromatic Molecules*; Wiley-Interscience: New York, 1970.
- (24) Ware, W. R. *J. Phys. Chem.* **1962**, *66*, 455–458.
- (25) Hautala, R. R.; Schore, N. E.; Turro, N. J. *J. Am. Chem. Soc.* **1973**, *95*, 5508–5514.
- (26) Pownall, H. J.; Smith, L. C. *Biochemistry* **1974**, *13*, 2594–2597.
- (27) Quina, F. H.; Toscano, V. G. *J. Phys. Chem.* **1977**, *81*, 1750–1754.
- (28) Sepulveda, L.; Lissi, E.; Quina, F. *Adv. Colloid Interface Sci.* **1986**, *25*, 1–57.
- (29) Gehlen, M.; De Schryver, F. C. *Chem. Rev.* **1993**, *93*, 199–221.
- (30) Almgren, M.; Grieser, F.; Thomas, J. K. *J. Am. Chem. Soc.* **1979**, *101*, 279–291.
- (31) Zana, R. *Surfactant Solutions: New Method of Investigation*; Marcel Dekker: New York and Basel, 1987.
- (32) Bacaloglu, R.; Bunton, C. A.; Ortega, F. J. *J. Phys. Chem.* **1989**, *93*, 1497–1502.
- (33) Moroi, Y. *J. Phys. Chem.* **1980**, *84*, 2186–2190.
- (34) Yekta, A.; Aikawa, M.; Turro, N. J. *Chem. Phys. Lett.* **1979**, *63*, 543–548, and the private communication with Dr. Turro.
- (35) Kalayanasundaram, K.; Thomas, J. K. *J. Am. Chem. Soc.* **1977**, *99*, 2039–2041.
- (36) Yoshida, N.; Takechi, M.; Asano, T.; Moroi, Y.; Humphry-Baker, B.; Graetzel, M. *Chem. Phys. Lett.* **2000**, *332*, 265–270.
- (37) Ham, J. S. *J. Chem. Phys.* **1953**, *21*, 756–758.
- (38) Durocher, G.; Sandorfy, C. *J. Mol. Spectrosc.* **1966**, *20*, 410–424.
- (39) Koyanagi, M. *J. Mol. Spectrosc.* **1968**, *25*, 273–290.
- (40) Nakashima, K.; Tanaka, I. *Langmuir* **1993**, *9*, 90–95.